

Cigarette smoke or motor vehicle exhaust exposure induces PD-L1 upregulation in lung epithelial cells in COPD model rats.

Rui Chen

Southern Medical University

Defu Li (✉ 850132932@qq.com)

Guangzhou Medical University <https://orcid.org/0000-0002-6795-375X>

Lingling Wang

PLA General Hospital of Southern Theatre Command: People's Liberation Army General Hospital of Southern Theatre Command

Jiahui Dong

PLA General Hospital of Southern Theatre Command: People's Liberation Army General Hospital of Southern Theatre Command

Richeng Xiong

PLA General Hospital of Southern Theatre Command: People's Liberation Army General Hospital of Southern Theatre Command

Zhenhui Guo

PLA General Hospital of Southern Theatre Command: People's Liberation Army General Hospital of Southern Theatre Command

Wenjie Huang

Southern Medical University <https://orcid.org/0000-0003-3915-7198>

Research Article

Keywords: COPD, lung cancer, PD-L1, CS, MVE, PM2.5

Posted Date: April 2nd, 2021

DOI: <https://doi.org/10.21203/rs.3.rs-250061/v1>

License:   This work is licensed under a Creative Commons Attribution 4.0 International License.

[Read Full License](#)

Abstract

Cigarette smoking and ambient air pollution are common risk factors for COPD and lung cancer. However, the underlying mechanism between COPD prevalence and lung cancer is remained elusive. In this study, we established rat COPD model through exposure to cigarette smoke (CS) or motor vehicle exhaust (MVE). The model rats developed COPD-like phenotypes, manifested as lung functions decline, lung inflammation and airway remodeling. The Programmed death-ligand 1 (PD-L1), a factor contributing to immune escape of tumor cells, was overexpressed in lungs from COPD model rats. The inflammatory responses and PD-L1 upregulations were also observed in cultured human bronchial epithelial cells BEAS-2B upon treatment with cigarette smoke extract (CSE) or diesel related particulate matter 2.5 (PM_{2.5}, SEM1650b). Furthermore, both CS/CSE and MVE/PM_{2.5} induced ERK1/2 activation, a kinase mediating PD-L1 upregulation in premalignant bronchial cells or NSCLC cells, in COPD rats' lungs or in BEAS-2B cells. Activations of STAT1/3, which was reportedly associated with PD-L1 expression in lung tumors, were detected in lungs from CS- or MVE-induced COPD model rats. However, CSE preferred to activate STAT3 and PM_{2.5} inclined to activate STAT1 in BEAS-2B cells. Therefore, we proposed that cigarette smoke and ambient air pollution elevate the risk of lung cancer in COPD patients by increasing PD-L1 expression in lung epithelial cells, suggesting the effects of immunosuppressive microenvironment on promoting tumorigenesis in COPD patient's lung.

Headings

What is the central question of this study?

Our study presented the effects of cigarette smoke and air pollutant on establishing COPD animal models with simultaneous PD-L1 upregulation in lung and suggested the premalignant PD-L1 upregulation in lung epithelial cells could be the link between COPD prevalence and lung cancer.

What is the main finding and its importance?

PD-L1 upregulation in airway epithelial cells exposed to various COPD risk factors might be associated with activation of ERK1/2 and alternative STAT family members.

Introduction

Several epidemiological studies indicated the link between COPD and lung cancer, including the association between airflow limitation and increased lung cancer incidence and mortality (1). Further study indicated the prevalence of COPD in lung cancer cases was independent of age, sex or smoking history (2). The main risk factors for COPD include but are not limited to cigarette smoke exposure and ambient air pollution, both of which are common risk factors for lung cancer, though the operative mechanisms between COPD prevalence and lung cancer are remained elusive (3-5).

Transmembrane protein Programmed death-ligand1 (PD-L1) is overexpressed in many cancer types including lung cancer. PD-L1 inhibited the functions of activated cytotoxic CD8⁺ T cells through interaction with PD-1 on cell surface of T cells (6). PD-L1 overexpression was supposed contribute to lung cancer initiation by facilitating immune escape in premalignant human bronchial epithelial cells (7). Clinical study showed that immunotherapy targeting on immune-checkpoint proteins PD-1/PD-L1 displayed promising clinical effects on non-small cell lung cancer (8). The associations among COPD, PD-1/PD-L1 axis activation and lung cancer therapy were revealed in clinical trial that immune checkpoint inhibitors (ICIs) displayed better therapeutic outcome in lung cancer patients underlying COPD than those without COPD (9). It was proposed that chronic lung inflammations commonly seen in COPD patients enhance the risk of tumorigenesis by weakening immune surveillance in lung. This hypothesis was partially verified by the findings that lipopolysaccharide (LPS) -mediated chronic inflammation upregulated PD-L1 expression through TLR4/ERK axis in lung cancer cells, or activated PD-1/PD-L1 axis in lung cancer model mice lung in which therapy coupled with anti-PD-1 treatment elicited better anti-tumor efficacy (10,11).

As the main risk factors for COPD, both CS and MVE exposure induced lung inflammation in COPD rodent animal models (12,13). However, the PD-L1 overexpression in COPD rodent animals has not been fully studied. Tobacco smoke was reported inducing PD-L1 increases in lung of A/J mice, a mouse strain having comparatively high lung tumor rate upon carcinogen treatments (14). Furthermore, although the air pollutant particles activated some proteins, such as ERK1/2 and STAT, being able to promote PD-L1 expression in bronchial epithelial cells or lung tumor cells, whether air pollutants affected lung PD-L1 expression in COPD patients or in COPD rodent animals are not fully explored (7,15-17).

In this study, we established rat COPD models through exposure to CS or MVE mimicking air pollution and reported that PD-L1 was upregulated in lung tissues from the two types of COPD model rats. PD-L1 levels in cultured human bronchial epithelial cells BEAS-2B were increased by CSE or diesel related PM_{2.5} in relative low dosage unable to induce obvious cytotoxicity. In lung tissues and cells, PD-L1 was upregulated along with the activation of ERK and STAT. A preferential pattern of activation of STAT family members was found in BEAS-2B cells upon CSE or PM_{2.5} stimulation. Our findings gave a clue that PD-L1 upregulation induced by cigarette smoking or air pollution in lung epithelial cells might contribute to the increased lung cancer incidence in COPD patients.

Methods And Materials

Animals

Male SD rats (8-12 weeks old) were purchased from the Guangdong Medical Laboratory Animal Center (Guangzhou, China). Rats were housed in the specific pathogen-free facilities and accessed to food and water freely. The experimental methods were approved by the Ethics Committee for Animal Experiments of the General Hospital of Southern Theater Command of PLA. For cigarette smoke exposure, the rats were randomly divided into two groups, the normal control group (CTL-CS) and cigarette smoke exposure

group (CS) and exposed to cigarette smoke according to previous method (13). Briefly, the rats were exposed to CS (9 cigarettes/h, 2 h per exposure, twice per day, 6 days per week) generated by Plum brand cigarette (produced by Guangdong Tobacco Industry Co., Ltd., China) in a whole body exposure chamber for 24 weeks. Each cigarette yields 11 mg tar, 1.0 mg nicotine, and 13 mg carbon monoxide (CO). For motor vehicle exhaust (MVE) exposure, rats were randomly divided into control group (CTL-MVE) and MVE exposure (MVE) group. MVE was given to the rats according to the previous protocol with modifications (12). Briefly, MVE was generated by using China standard 95# gasoline and exposed to rats (2 h per session, 3 sessions per day, 6 days per week) in a MVE exposure system for 24 weeks.

Bronchoalveolar lavage fluid (BALF) collection

Rat's right lung was lavaged with 4 ml saline for one time. Total BALF was collected and centrifuged at 500 g for 10 min at 4°C to pellet the cells. The cell pellets were re-suspended in 1 ml saline for total cell counting using a hemocytometer. The cells were then subjected to Giemsa staining for differential counting of neutrophils, macrophages and lymphocytes. The supernatant was stored at -80°C for detecting the pro-inflammatory cytokines.

Lung function measurement

The rats exposed to CS or MVE were subjected to lung function measurement by using a Forced Pulmonary Maneuver System (Buxco Research Systems, Wilmington, NC, USA) following a protocol described previously (13). The values of parameters airway resistance, chord compliance, total lung capacity and the ratio of FEV50/FVC were determined.

Histological staining and Morphometry

After sacrifice, the left lungs were fixed with 4% PFA, embedded with paraffin and sectioned into 4 µm slices. Then the slices were subjected to H&E staining for histological evaluation and to PAS staining for goblet cells hyperplasia evaluation by using software Image-Pro Plus version 6.0 (Media Cybernetics, Rockville, MD, USA). Alveolar enlargement and destruction were evaluated by the mean linear intercept (Lm) assessed by calculating the ratio of total alveolar length to the number of alveoli per unit area under microscopy. The ratio of wall area to the total bronchial area was determined and scored according to our previously described method (18). The PAS-positive area and total area of corresponding bronchial epithelium were measured as previously described method (19). Each calculation mentioned above was based on five representing slides across different regions of the lung.

Cell culture

Human bronchial epithelial cells BEAS-2B were purchased from JENNIO biological technology (Guangzhou, China) and cultured in DMEM medium containing 10% FBS, 100 U/mL penicillin and 100 µg/mL streptomycin in a humidified incubator at 37 °C with 95% (v/v) air and 5% (v/v) CO₂. The cigarette smoke extract (CSE) was prepared freshly according to a previously reported method and used to treat

cells in concentration ranged from 0 to 20% in medium containing 1% FBS for 48 h (13). For PM_{2.5} treatment, the cells were serum starved for 12 h and then exposed to 0-300 µg/ml PM_{2.5} Standard Reference DEP material - SRM 1650b (National Institute of Standards and Technology (NIST), China) dissolved in medium containing 1% FBS for 48 h. Cell viability was determined by using a CCK-8 test kit and presented as percentage of control.

Quantitative RT-PCR assay

Total RNA was extracted from lung tissues or cultured cells and reversely transcribed into cDNA by using the PrimeScript RT reagent Kit with gDNA Eraser (TAKARA, Japan). The relative mRNA levels of PD-L1 were quantified by using iCycler iQ RT-PCR Detection System (Bio-Rad Laboratories Inc., United States) with following primers (rat PD-L1 (forward:5'- GGAATGCAGATTCCCAGTAGAA-3'; reverse: 5'- CTCTCCCTCCACAACTGAATAA-3'); rat GAPDH (forward: 5'-GACATGCCGCCTGGAGAAAC-3'; reverse: 5'- AGCCCAGGATGCCCTTTAGT-3'); human PD-L1 (forward: 5'-CAATGTGACCAGCACACTGAGAA-3'; reverse: 5'-GGCATAATAAGATGGCTCCCAGAA-3') and human GAPDH (forward: ; 5'-CCCACTCCTCCACCTTTGAC-3'; reverse: 5'-CCACCACCCTGTTGCTGTAG-3')). Relative mRNA levels for PD-L1 were normalized to the results of GAPDH and expressed as percentage of control.

Western blotting

The total protein was extracted from the lung tissues or cultured cells by homogenizing in RIPA lysis buffer containing 1% protease inhibitor cocktail (Sigma-Aldrich). Equal amounts of protein from each sample were separated in SDS-PAGE and blotted with the following primary antibodies and corresponding secondary antibodies. Antibodies against PD-L1 (13684S), ERK1/2 (4695S), phosphorylated ERK1/2 (8544S), were obtained from Cell Signaling Technology (Beverly, MA, USA). Antibodies against Gapdh (ab8245), STAT1 (ab31369), phosphorylated STAT1 (ab109461), STAT3 (ab68153) and phosphorylated STAT3 (ab76315) were obtained from Abcam (Cambridge, UK). The blotted bands were developed by using an Immun-Star HRP chemiluminescent kit (Bio-Rad Laboratories), imaged by Tanon 5200 Chemiluminescence Imaging System (Shanghai Tanon Science & Technology, Shanghai, China) and semi-quantitated by using the software Image J.

Immunofluorescence microscopy

Paraffin sections of lung tissues were deparaffinised in xylene, rehydrated and antigen retrieved in boiling citrate buffer. Cultured cells were seeded on cover slides, treated with CSE or PM_{2.5} and fixed with 4% PFA. Then the lung tissue sections or cells were incubated with PD-L1 antibody overnight at 4°C followed by fluorescence-labeled secondary antibody and nuclear counterstain dye DAPI (Sigma-Aldrich). Images were captured by a fluorescence microscope.

ELISA

The ELISA kits from eBioscience (San Diego, CA, USA) were used to measure the levels of rat IL6 (88-50625) and rat TNF- α (88-7340) in BALF and the levels of human IL6 (88-7066) and human IL8 (88-8086) in cell culture medium according to the manufacturer's instructions. The levels of Muc5ac in BALF were measured by using a capture antibody for Muc5ac (sc-21701, Santa Cruz Biotechnology, CA) and corresponding detection antibody obtained from KPL, Inc. (Gaithersburg, MD, USA) according to protocol described previously (20).

Statistical analysis

All *in vitro* experiments were carried out in triplicate and repeated three times. Comparison between two groups were determined by Students *t*-test, one-way ANOVA further followed by Bonferroni post-hoc test was adopted for comparison in experiments with ≥ 3 groups. SPSS v. 16.0 and Graphpad prism 5.0 were used for statistics and graphing, respectively. Data were presented as mean \pm SEM. N denotes the number of repeats in cell experiments or the number of animals. *P* values less than 0.05 or 0.01 were considered as statistically significant or extremely statistically significant respectively in all cases.

Results

COPD-like symptoms developed in rats exposed to CS or MVE.

The COPD-like symptoms were observed in rats exposed to CS or MVE. The lung functions were declined in rats exposed to CS or MVE indicated by the significantly increased parameters of resistance, chord compliance and total lung capacity, and the decreased ratios of FEV50/FVC when compared with those rats in respective control group (Fig. 1A). The mean linear intercept values, a histological measure of lung damage, were also increased in rats exposed to CS or MVE (Fig. 1B). Furthermore, significant differences were observed in parameters resistance, total lung capacity, FEV50/FVC and mean linear intercept value between CS and MVE exposed rats, revealed more severe lung damage in CS exposed rats.

The inflammatory responses developed in lungs from rats exposed to CS or MVE, manifested by increased leukocytes and pro-inflammatory cytokine levels in BALF. When compared CS- with MVE-exposed rats, we found although CS-exposed rats had much more inflammatory cells in BAL fluid than MVE-exposed rats ($P < 0.01$), the levels of proinflammatory cytokines IL-6 ($P < 0.05$) and TNF- α ($P > 0.1$) in BAL fluid did not show similarly obvious difference between the two COPD models (Fig 2A and B). Mucus hypersecretion in model rats was characterized by goblet cell hyperplasia indicated by positive PAS staining and upregulated Muc5ac levels in BALF. In the two COPD models, CS exposure induced more obvious mucus hypersecretion than MVE exposure (Fig 2C-D). Furthermore, the increased ratios of wall area/total bronchial area were seen in both COPD models, though no difference existed between them (Fig 2E). It meant that the two COPD models presented the same extent in airway remodeling.

PD-L1 upregulations in lungs exposed to CS or MVE

The lysates of lung tissues were subjected to quantitative RT-PCR or western blotting for measurements of mRNA or protein levels of PD-L1. As shown in figure 3A and B, both mRNA and protein levels of PD-L1 were upregulated in rats' lungs exposed to CS or MVE. However, concerning the changes of PD-L1 mRNA or protein levels, no difference existed between the two groups of COPD model rats. Immunofluorescence staining with antibody against PD-L1 indicated PD-L1 predominantly expressed in bronchial epithelial cells. When compared with the normal rats, we observed more cells with increased immunofluorescence staining in sections of COPD model rats' lungs (Fig. 3C).

Both CSE and PM_{2.5} induced inflammatory responses in lung epithelial cells

In order to investigate the effects of CS or MVE exposure on bronchial epithelial cells, we treated the cultured immortal normal human bronchial epithelial cells BEAS-2B with cigarette smoke extracts (CSE) or diesel related PM_{2.5} which mimicked the effects of MVE. Both CSE and PM_{2.5} in high levels, namely more than 10% for CSE and more than 200 µg/ml for PM_{2.5}, reduced cell viability for more than 50% (Fig 4A-B). In order to avoid cytotoxicity, we used 2% CSE or 100 µg/ml PM_{2.5} in cell treatments hereafter. In these dosages, both CSE and PM_{2.5} induced inflammatory responses in BEAS-2B cells manifested by upregulated cytokine levels of IL-6 and IL-8 in cell culture medium. Moreover, CSE induced more robust productions of IL-6 and IL-8 than PM_{2.5} (Fig 4C-D).

PD-L1 upregulations in bronchial epithelial cells treated with CSE or PM_{2.5}

Both CSE and PM_{2.5} enhanced PD-L1 expression in mRNA and protein levels in BEAS-2B cells. The mRNA and protein levels of PD-L1 were higher in cells exposed to CSE than those cells exposed to PM_{2.5} (Fig 5A-B). The upregulations of PD-L1 induced by CSE or PM_{2.5} were confirmed by the immunofluorescence staining (Fig. 5C).

***In vitro* and *in vivo* activation of ERK and STAT upon CS/CSE or MVE/ PM_{2.5} exposure**

The signaling mediated by ERK or STAT was activated in lung from COPD model rats. Here we found that both CS and MVE induced phosphorylations of ERK1/2, STAT1 and STAT3 in lung tissues from the two rat COPD models we employed, though only phosphorylations of ERK1/2 showed difference between the two model types (Fig6 A). In cultured cells, both CSE and PM_{2.5} induced very obvious ERK1/2 phosphorylation. However, CSE preferred to induce STAT3 but not STAT1 phosphorylation, whereas PM_{2.5} inclined to induce STAT1 phosphorylation in BEAS-2B cells (Fig 6B).

Discussion

In the present study, we established COPD model with rats, an animal model without hypersensitivity to lung tumorigenesis induction, by CS or MVE exposure. The COPD model rats displayed typical COPD-like phenotypes, including lung functions decline and lung inflammations, paralleled with PD-L1 upregulation in lung. Concentrated PD-L1 was distributed in bronchial epithelial cells. The PD-L1 upregulation was also

induced by CSE or diesel related PM_{2.5} in bronchial epithelial cells BEAS-2B. ERK1/2 and STAT1/3, both of which reportedly modulated PD-L1 expression in lung cancer cells, were activated upon CS/CSE or MVE/PM_{2.5} treatments in lung tissues or in bronchial epithelial cells. Together, our results gave clue that premalignant PD-L1 upregulation in lung epithelial cells could be the link between COPD prevalence and lung cancer.

The increase of PD-1/PD-L1 axis in lung cancer generally exhibited the upregulated expressions of PD-1 in T cells and of PD-L1 in tumor cells which lead to immune escape of tumor cells (21,22). The main immunological dysfunction in COPD patients' lung is T-cell exhaustion due to the binding of immune checkpoints on T-cells. The interaction of PD-1/PD-L1 established an immunosuppressive microenvironment facilitating the tumor initiation, development and progression (23). However, despite the increased CD8⁺ PD1 levels in COPD patients' lung (24), at least one study mentioned no difference found in CD4/8⁺ T cells PD-1 levels in resected tumor tissues between COPD and non-COPD NSCLC patients (9). Therefore, PD-L1 overexpression in lung epithelial cells is critical for establishment of immune escape contributing to increased lung cancer incidence in COPD patients.

By comparing the status of lung functions decline, the airway inflammation and lung PD-L1 upregulations between the two COPD models, we noticed that more severe lung functions decline and more airway leucocytes infiltration did not bring higher PD-L1 expressions in lung. Concerning the PD-L1 overexpression in NSCLC cells, one point of view supposed the PD-L1 overexpression was modulated by crosstalk between NSCLC and activated macrophages (17). In a study focusing on relationship between PD-L1 expressions and immune cells distribution in resected lung cancer tissues, tumor PD-L1 expression was found associated with the tumor infiltrated macrophages which accumulate around PD-L1-positive carcinoma cell areas in early lung adenocarcinoma patients. The cytokines secreted by tumor associated macrophages, including TGF-β1, TNF-α, IL-10, IL-1α, IL-1β and IL-27, are supposed to be extrinsic regulator of tumor PD-L1 expression and contribute to tumor development in early stage (25). However, in our study, the PD-L1 levels in lung were similar between the two models, though CS exposed rats had much more airway macrophages, which reflected that the increased number of airway macrophages might correlate with PD-L1 upregulation but more airway macrophages might not mean higher lung PD-L1 expression in COPD (Fig1-3). One cohort study supported the viewpoint that IL-1β level in peripheral blood is correlated with PD-L1 expression in lung tumor tissues and poor prognosis of lung cancer. And the levels of IL-6 and TNF-α are associated with the level of IL-1β (26). Compared with the extent of lung functions decline or airway leukocytes number, we doubted whether the increase of airway proinflammatory cytokine levels is more consistent with PD-L1 upregulation. As indicator of airway inflammation, the proinflammatory cytokine levels in BAL fluid represented by TNF-α and IL-6 did not show extremely significant difference between the two models (Fig. 2B). The association between proinflammatory cytokine levels and PD-L1 expression level of lung epithelial cells was obvious in cultured BEAS-2B cells exposed to CS or PM_{2.5}, a simpler system when compared with lung tissue, in which CS induced more secreted cytokines in culture medium and higher PD-L1 expression (Fig. 4C).

Therefore, we supposed the airway proinflammatory cytokine levels might be more suitable to indicate the lung PD-L1 overexpression than other parameters in COPD.

Our results showed that the ratio of p-ERK/ERK, a hallmark of lung inflammation, was increased in COPD rats' lungs and in cultured bronchial epithelial cells upon CSE or diesel related PM_{2.5} treatments. Other studies also indicated *in vivo* and *in vitro* phosphorylation of ERK was triggered by CS/CSE or diesel related PM_{2.5} in bronchial epithelial cells or in lung cancer cells (27-29). Unlike previously report in which PM_{2.5} induced phosphorylation of ERK in bronchial epithelial cells in dosage bringing cell cycle arrest (30), our results showed that both CSE and diesel related PM_{2.5} activated ERK and upregulated PD-L1 in relative low dosage without inducing obvious cell viability loss but enough to induce inflammatory responses (Fig. 4 and 5). The carcinogens in cigarette smoke like polycyclic aromatic hydrocarbon (PAHs), or PM_{2.5} bound PAHs were supposed induced ERK activation and cell transformation in bronchial epithelial cells (15,31). It should be noted that higher p-ERK/ERK ratio in lungs found in CS-COPD rats did not bring consequently further PD-L1 overexpression (Fig. 6). In culture cells received with CSE or PM_{2.5} treatment, more robust increase of PD-L1 even emerged in CSE treated cells in spite of less p-ERK augment. Thus, we supposed p-ERK is correlated with PD-L1 upregulation in COPD lung epithelial cells. But PD-L1 expression is probably modulated by elements unlimited to p-ERK.

The phosphorylation of STAT1 and 3 were detected in lungs from both COPD rat models. No difference existed between CS and MVE in promoting STAT1 and 3 phosphorylation in lung. However, in cultured bronchial epithelial cells BEAS-2B, CSE or PM_{2.5} activated STAT family members preferentially, namely STAT3 for CSE and STAT1 for PM_{2.5}. It is not known whether the difference in PD-L1 levels between CSE and PM_{2.5} treatment was due to alternative activation of STAT family members. Actually, conflicting results have been obtained regarding the involvement of p-STAT in modulating PD-L1 expression in lung epithelial cells. It might depend on the types of stimulant and the cell types. Cigarette smoke carcinogen NNK induced PD-L1 expression in lung tumors through IFN γ /STAT1/STAT3 signaling axis (17). Cytokine IFN-gamma triggers PD-L1 expression in lung cancer cells through JAK/STAT1 or JAK/STAT3 pathway (32,33). Nevertheless, in a cellular model for viral infection in lung epithelial cells, IL-22 prohibited PD-L1 upregulation in a STAT3 activation dependent manner (34). Our results firstly reported diesel related PM_{2.5} preferentially activated STAT1 paralleled with PD-L1 upregulation in bronchial epithelial cells. Further research is needed to explore the effects of STAT phosphorylation on PD-L1 upregulation in COPD developed from various risk factors.

In conclusion, our study presented the effects of cigarette smoke and air pollutant on establishing COPD animal models with simultaneous PD-L1 upregulation in lung and suggested the premalignant PD-L1 upregulation in lung epithelial cells could be the link between COPD prevalence and lung cancer. Additionally, PD-L1 upregulation in airway epithelial cells exposed to various COPD risk factors might be associated with activation of ERK1/2 and alternative STAT family members.

Abbreviations

COPD, Chronic obstructive pulmonary disease; CS, cigarette smoke; MVE, motor vehicle exhaust; CSE, cigarette smoke extract; PM_{2.5}, particulate matter 2.5; PD-L1, programmed death-ligand 1; ERK, extracellular regulated protein kinases; STAT, signal transducer and activator of transcription; BALF, bronchoalveolar lavage fluid

Declarations

Funding

This study was supported by grants from the National Natural Science Foundation of China (81900033), Natural Science Foundation of Guangdong Province (2018A030313787).

Availability of data and material

This manuscript or the results included are original and have not been submitted for publication elsewhere.

Conflict of interest

The authors have no conflict of interest to declare

Author contributions

Wenjie Huang conceived the idea for the project. Zhenhui Guo contributed to the design of the protocol. Rui Chen and Defu Li built the animal models, collected samples and drafted the manuscript. Lingling Wang analysed the data. Jiahui Dong and Richeng Xiong took part in the collection of samples. Wenjie Huang revised the manuscript critically. All authors approved the final version of the manuscript and agree to be accountable for all aspects of the work in ensuring that questions related to the accuracy or integrity of any part of the work are appropriately investigated and resolved. All persons designated as authors qualify for authorship, and all those who qualify for authorship are listed.

Ethics approval

The experimental methods were approved by the Ethics Committee for Animal Experiments of the General Hospital of Southern Theater Command of PLA

Acknowledgments

We would like to thank Professor Wenju Lu for technical assistance in the establishment of MVE-induced COPD animal models.

Consent for publication

All authors have read the manuscript and approved the submission.

References

- 1 Tockman, M. S., Anthonisen, N. R., Wright, E. C., and Donithan, M. G. 1987. Airways obstruction and the risk for lung cancer. *Ann Intern Med* 106:512.
- 2 Young, R. P., Hopkins, R. J., Christmas, T., Black, P. N., Metcalf, P., and Gamble, G. D. 2009. COPD prevalence is increased in lung cancer, independent of age, sex and smoking history. *Eur Respir J* 34:380.
- 3 Fajersztajn, L., Veras, M., Barrozo, L. V., and Saldiva, P. 2013. Air pollution: a potentially modifiable risk factor for lung cancer. *Nat Rev Cancer* 13:674.
- 4 Hecht, S. S. 1999. Tobacco smoke carcinogens and lung cancer. *J Natl Cancer Inst* 91:1194.
- 5 Wang, C., Xu, J., Yang, L., Xu, Y., Zhang, X., Bai, C., Kang, J., Ran, P., Shen, H., Wen, F., Huang, K., Yao, W., Sun, T., Shan, G., Yang, T., Lin, Y., Wu, S., Zhu, J., Wang, R., Shi, Z., Zhao, J., Ye, X., Song, Y., Wang, Q., Zhou, Y., Ding, L., Chen, Y., Guo, Y., Xiao, F., Lu, Y., Peng, X., Zhang, B., Xiao, D., Chen, C. S., Wang, Z., Zhang, H., Bu, X., An, L., Zhang, S., Cao, Z., Zhan, Q., Yang, Y., Cao, B., Dai, H., Liang, L., and He, J. 2018. Prevalence and risk factors of chronic obstructive pulmonary disease in China (the China Pulmonary Health [CPH] study): a national cross-sectional study. *Lancet* 391:1706.
- 6 Pardoll, D. M. 2012. The blockade of immune checkpoints in cancer immunotherapy. *Nat Rev Cancer* 12:252.
- 7 Lee, M. H., Yanagawa, J., Tran, L., Walser, T. C., Bisht, B., Fung, E., Park, S. J., Zeng, G., Krysan, K., Wallace, W. D., Paul, M. K., Girard, L., Gao, B., Minna, J. D., Dubinett, S. M., and Lee, J. M. 2020. FRA1 contributes to MEK-ERK pathway-dependent PD-L1 upregulation by KRAS mutation in premalignant human bronchial epithelial cells. *Am J Transl Res* 12:409.
- 8 Jia, M., Feng, W., Kang, S., Zhang, Y., Shen, J., He, J., Jiang, L., Wang, W., Guo, Z., Peng, G., Chen, G., and Liang, W. 2015. Evaluation of the efficacy and safety of anti-PD-1 and anti-PD-L1 antibody in the treatment of non-small cell lung cancer (NSCLC): a meta-analysis. *J Thorac Dis* 7:455.
- 9 Mark, N. M., Kargl, J., Busch, S. E., Yang, G. H. Y., Metz, H. E., Zhang, H., Hubbard, J. J., Pipavath, S. N. J., Madtes, D. K., and Houghton, A. M. 2018. Chronic Obstructive Pulmonary Disease Alters Immune Cell Composition and Immune Checkpoint Inhibitor Efficacy in Non-Small Cell Lung Cancer. *Am J Respir Crit Care Med* 197:325.
- 10 Kang, X., Li, P., Zhang, C., Zhao, Y., Hu, H., and Wen, G. 2020. The TLR4/ERK/PDL1 axis may contribute to NSCLC initiation. *Int J Oncol* 57:456.
- 11 Liu, C. H., Chen, Z., Chen, K., Liao, F. T., Chung, C. E., Liu, X., Lin, Y. C., Keohavong, P., Leikauf, G. D., and Di, Y. P. 2020. Lipopolysaccharide-mediated chronic inflammation promotes tobacco carcinogen-induced lung cancer and determines the efficacy of immunotherapy. *Cancer Res*.

- 12 Shu, J., Lu, W., Yang, K., Zheng, Q., Li, D., Li, Y., Kuang, M., Liu, H., Li, Z., Chen, Y., Zhang, C., Luo, X., Huang, J., Wu, X., Tang, H., and Wang, J. 2018. Establishment and evaluation of chronic obstructive pulmonary disease model by chronic exposure to motor vehicle exhaust combined with lipopolysaccharide instillation. *Exp Physiol* 103:1532.
- 13 Li, D., Wang, J., Sun, D., Gong, X., Jiang, H., Shu, J., Wang, Z., Long, Z., Chen, Y., Zhang, Z., Yuan, L., Guan, R., Liang, X., Li, Z., Yao, H., Zhong, N., and Lu, W. 2018. Tanshinone IIA sulfonate protects against cigarette smoke-induced COPD and down-regulation of CFTR in mice. *Sci Rep* 8:376.
- 14 Wang, G. Z., Zhang, L., Zhao, X. C., Gao, S. H., Qu, L. W., Yu, H., Fang, W. F., Zhou, Y. C., Liang, F., Zhang, C., Huang, Y. C., Liu, Z., Fu, Y. X., and Zhou, G. B. 2019. The Aryl hydrocarbon receptor mediates tobacco-induced PD-L1 expression and is associated with response to immunotherapy. *Nat Commun* 10:1125.
- 15 Chen, S., Li, D., Zhang, H., Yu, D., Chen, R., Zhang, B., Tan, Y., Niu, Y., Duan, H., Mai, B., Yu, J., Luan, T., Chen, L., Xing, X., Li, Q., Xiao, Y., Dong, G., Aschner, M., Zhang, R., Zheng, Y., and Chen, W. 2019. The development of a cell-based model for the assessment of carcinogenic potential upon long-term PM2.5 exposure. *Environ Int* 131:104943.
- 16 Xu, Z., Wu, H., Zhang, H., Bai, J., and Zhang, Z. 2020. Interleukins 6/8 and cyclooxygenase-2 release and expressions are regulated by oxidative stress-JAK2/STAT3 signaling pathway in human bronchial epithelial cells exposed to particulate matter $\leq 2.5 \mu\text{m}$. *J Appl Toxicol* 40:1210.
- 17 Narayanapillai, S. C., Han, Y. H., Song, J. M., Kebede, M. E., Upadhyaya, P., and Kassie, F. 2020. Modulation of the PD-1/PD-L1 immune checkpoint axis during inflammation-associated lung tumorigenesis. *Carcinogenesis* 41:1518.
- 18 Shu, J., Li, D., Ouyang, H., Huang, J., Long, Z., Liang, Z., Chen, Y., Zheng, Q., Kuang, M., Tang, H., Wang, J., and Lu, W. 2017. Comparison and evaluation of two different methods to establish the cigarette smoke exposure mouse model of COPD. *Sci Rep* 7:15454.
- 19 Li, D., Sun, D., Yuan, L., Liu, C., Chen, L., Xu, G., Shu, J., Guan, R., Xu, J., Li, Y., Yi, G., Yao, H., Zhong, N., Wang, J., and Lu, W. 2020. Sodium tanshinone IIA sulfonate protects against acute exacerbation of cigarette smoke-induced chronic obstructive pulmonary disease in mice. *Int Immunopharmacol* 81:106261.
- 20 Shao, M. X., Ueki, I. F., and Nadel, J. A. 2003. Tumor necrosis factor alpha-converting enzyme mediates MUC5AC mucin expression in cultured human airway epithelial cells. *Proc Natl Acad Sci U S A* 100:11618.
- 21 Aldarouish, M., Su, X., Qiao, J., Gao, C., Chen, Y., Dai, A., Zhang, T., Shu, Y., and Wang, C. 2019. Immunomodulatory effects of chemotherapy on blood lymphocytes and survival of patients with advanced non-small cell lung cancer. *Int J Immunopathol Pharmacol* 33:2058738419839592.

- 22 Kim, G. J., Lee, J. H., Park, W. J., Lee, H. W., Hwang, I. S., and Lee, D. H. 2019. The Prognostic Value of Measuring PD-L1 mRNA Expression Levels in Surgically Resected Non-Small Cell Lung Cancer. *Ann Clin Lab Sci* 49:317.
- 23 Chen, N., Fang, W., Lin, Z., Peng, P., Wang, J., Zhan, J., Hong, S., Huang, J., Liu, L., Sheng, J., Zhou, T., Chen, Y., Zhang, H., and Zhang, L. 2017. KRAS mutation-induced upregulation of PD-L1 mediates immune escape in human lung adenocarcinoma. *Cancer Immunol Immunother* 66:1175.
- 24 McKendry, R. T., Spalluto, C. M., Burke, H., Nicholas, B., Cellura, D., Al-Shamkhani, A., Staples, K. J., and Wilkinson, T. M. 2016. Dysregulation of Antiviral Function of CD8(+) T Cells in the Chronic Obstructive Pulmonary Disease Lung. Role of the PD-1-PD-L1 Axis. *Am J Respir Crit Care Med* 193:642.
- 25 Shima, T., Shimoda, M., Shigenobu, T., Ohtsuka, T., Nishimura, T., Emoto, K., Hayashi, Y., Iwasaki, T., Abe, T., Asamura, H., and Kanai, Y. 2020. Infiltration of tumor-associated macrophages is involved in tumor programmed death-ligand 1 expression in early lung adenocarcinoma. *Cancer Sci* 111:727.
- 26 Lim, J. U. and Yoon, H. K. 2020. Potential predictive value of change in inflammatory cytokines levels subsequent to initiation of immune checkpoint inhibitor in patients with advanced non-small cell lung cancer. *Cytokine* 138:155363.
- 27 Guan, R., Wang, J., Li, D., Li, Z., Liu, H., Ding, M., Cai, Z., Liang, X., Yang, Q., Long, Z., Chen, L., Liu, W., Sun, D., Yao, H., and Lu, W. 2020. Hydrogen sulfide inhibits cigarette smoke-induced inflammation and injury in alveolar epithelial cells by suppressing PHD2/HIF-1 α /MAPK signaling pathway. *Int Immunopharmacol* 81:105979.
- 28 Park, E. J., Park, Y. J., Lee, S. J., Lee, K., and Yoon, C. 2019. Whole cigarette smoke condensates induce ferroptosis in human bronchial epithelial cells. *Toxicol Lett* 303:55.
- 29 Blanchet, S., Ramgolam, K., Baulig, A., Marano, F., and Baeza-Squiban, A. 2004. Fine particulate matter induces amphiregulin secretion by bronchial epithelial cells. *Am J Respir Cell Mol Biol* 30:421.
- 30 Wu, J., Shi, Y., Asweto, C. O., Feng, L., Yang, X., Zhang, Y., Hu, H., Duan, J., and Sun, Z. 2017. Fine particle matters induce DNA damage and G2/M cell cycle arrest in human bronchial epithelial BEAS-2B cells. *Environ Sci Pollut Res Int* 24:25071.
- 31 Miller, A., Brooks, G. D., McLeod, L., Ruwanpura, S., and Jenkins, B. J. 2015. Differential involvement of gp130 signalling pathways in modulating tobacco carcinogen-induced lung tumourigenesis. *Oncogene* 34:1510.
- 32 Zhang, X., Zeng, Y., Qu, Q., Zhu, J., Liu, Z., Ning, W., Zeng, H., Zhang, N., Du, W., Chen, C., and Huang, J. A. 2017. PD-L1 induced by IFN-gamma from tumor-associated macrophages via the JAK/STAT3 and PI3K/AKT signaling pathways promoted progression of lung cancer. *Int J Clin Oncol* 22:1026.

33 Li, Y. M., Yu, J. M., Liu, Z. Y., Yang, H. J., Tang, J., and Chen, Z. N. 2019. Programmed Death Ligand 1 Indicates Pre-Existing Adaptive Immune Response by Tumor-Infiltrating CD8(+) T Cells in Non-Small Cell Lung Cancer. *Int J Mol Sci* 20.

34 Seki, N., Kan, O. K., Matsumoto, K., Fukuyama, S., Hamano, S., Tonai, K., Ota, K., Inoue, H., and Nakanishi, Y. 2017. Interleukin-22 attenuates double-stranded RNA-induced upregulation of PD-L1 in airway epithelial cells via a STAT3-dependent mechanism. *Biochem Biophys Res Commun* 494:242.

Figures

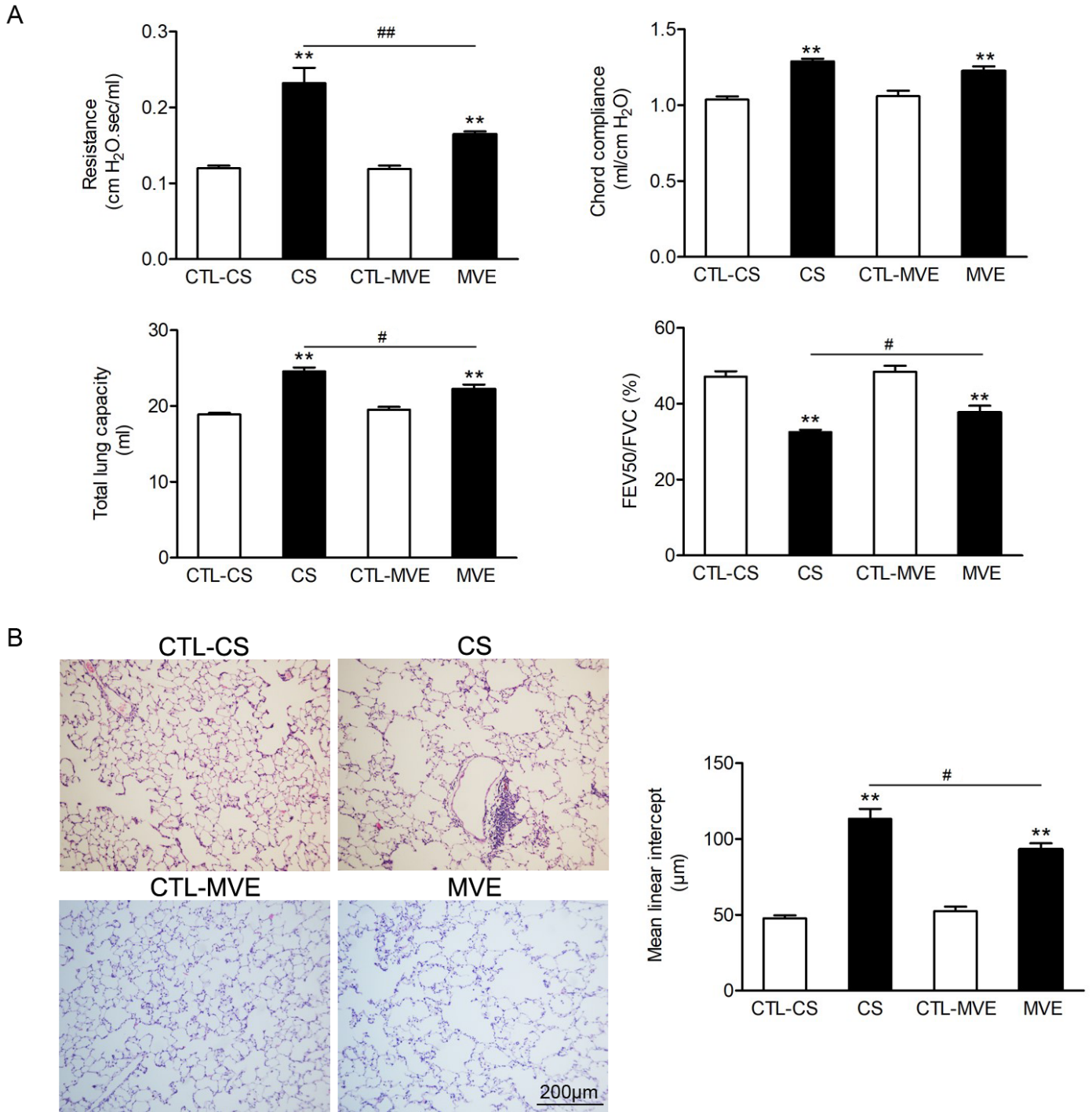


Figure 1

COPD like lung function loss was found in rats exposed to cigarette smoke or motor vehicle exhaust. Male SD rats were exposed to cigarette smoke (CS) for 60 days in a whole body exposure chamber or motor vehicle exhaust (MVE) in an exposure system for 24 weeks. (A) The values of lung function parameters, including airway resistance, chord compliance, total lung capacity and the ratio of FEV50/FVC were determined. (B) Representative H&E staining images of rat tissues sections with or without CS or MVE exposure treatment. Each calculation for mean linear intercept (Lm) in lung was

based on 6 rats and five representing slides across different regions of the lung from each rat. Data are represented as mean \pm SEM (n=6). **P < 0.01 for CS or MVE group versus respective CTL group; #P < 0.05 and ##P < 0.01 for CS group versus MVE group.

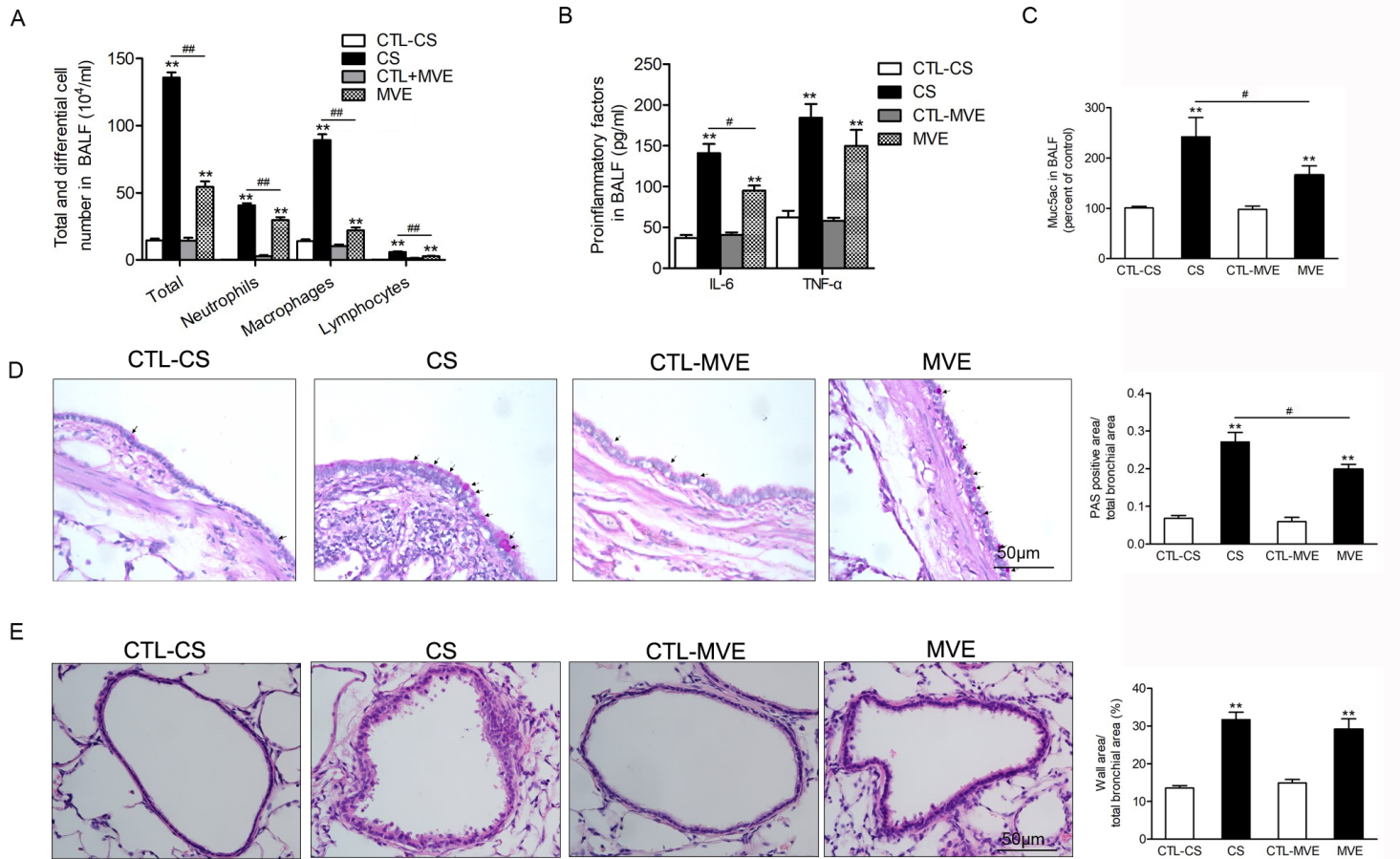


Figure 2

Cigarette smoke and motor vehicle exhaust exposure induced inflammation and mucus hypersecretion in airway. The bronchial alveolar lavage fluid (BALF) was collected. (A) The cells in BALF were separated, subjected to H&E staining and differential counting. (B) The levels of IL-6 and TNF- α in supernatants of BALF were determined with ELISA. (C) The Muc5AC levels in BALF supernatants were determined with ELISA. (D) The PAS staining of lung sections and the PAS staining positive areas in bronchia were semi-quantitatively analyzed and presented as ratios to the total bronchial area. (E) Lung sections were subjected to H&E staining and the calculation of bronchial wall area ratio to the total bronchial area. The ratio analyses for PAS staining positive area or bronchial wall area were performed in 6 rats per group with five representing slides in each rat. Data are represented as mean \pm SEM (n=6). **P < 0.01 for CS or MVE group versus respective CTL group; #P < 0.05 and ##P < 0.01 for CS group versus MVE group.

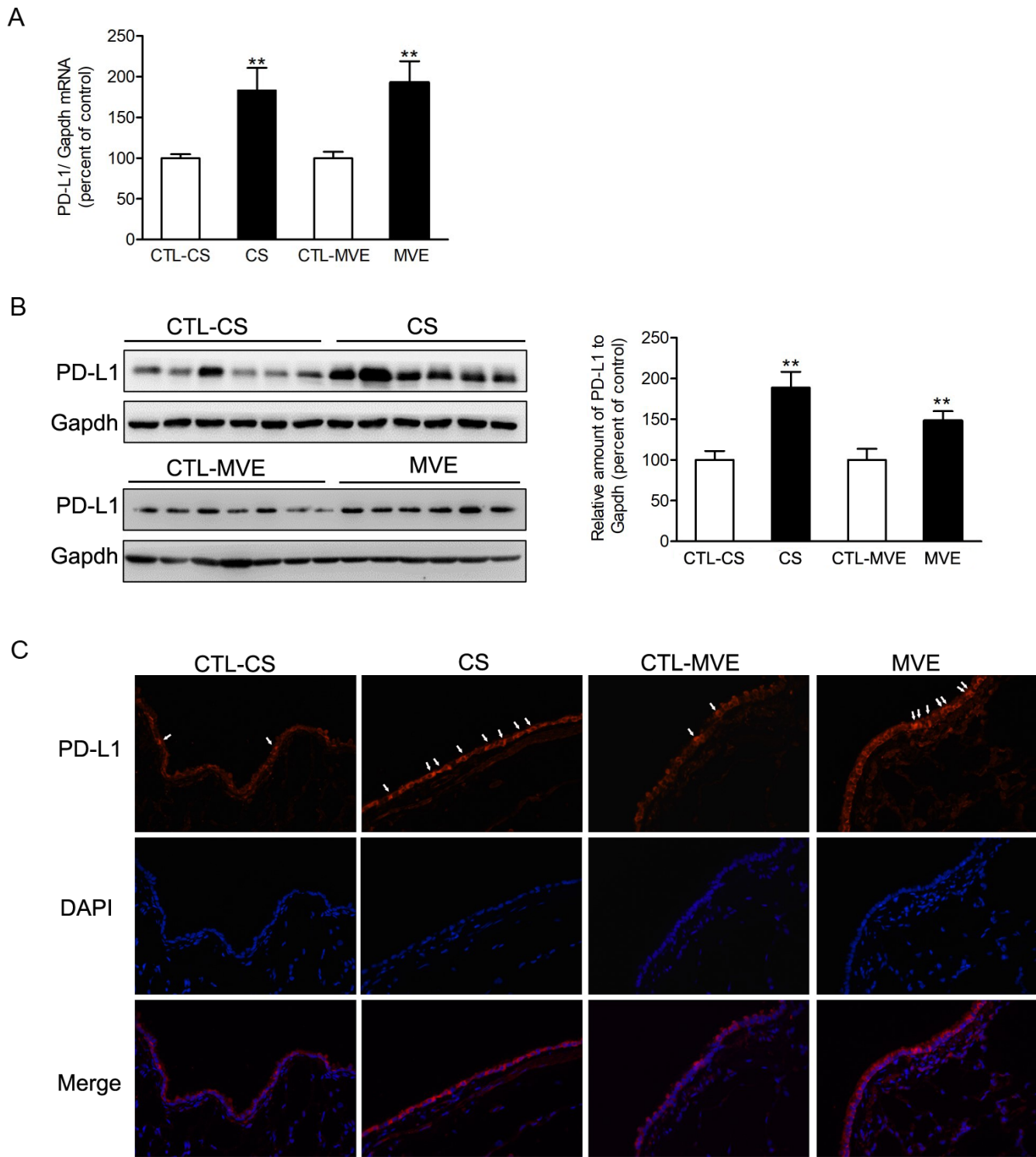


Figure 3

PD-L1 was increased in lung exposed to CS or MVE. (A) The relative mRNA levels of PD-L1 in lung tissues were presented as percentage of the control group. (B) Protein levels of PD-L1 in lung tissues were determined by using western blotting. The blotted bands were relatively semi-quantitated to internal control (GAPDH) by densitometry and presented as relative amount to control groups. Data are presented as mean \pm SEM. ** $P < 0.01$ for CS or MVE group versus respective CTL group. (C) Representative images

from lung tissue sections with immunofluorescence staining of PD-L1. Arrows indicated the cells with relatively brighter fluorescence staining than average.

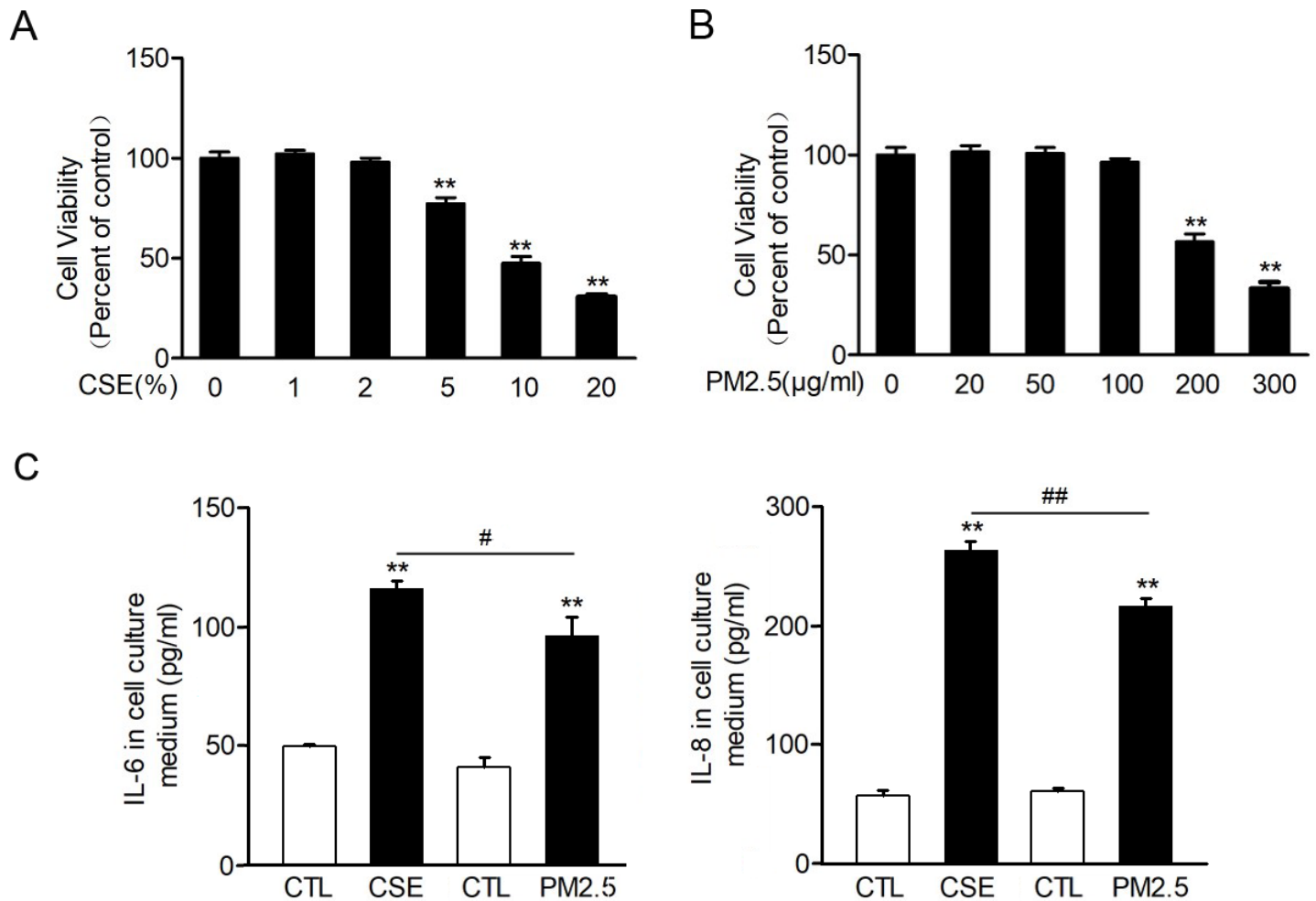


Figure 4

Cigarette smoke extract and PM2.5 reduced cell viability and induced proinflammatory cytokines production in airway epithelial cells. (A-B) Human normal bronchial cells BEAS-2B were incubated with 0-20% CSE or 0-300 µg/ml PM2.5 for 48 hr. Cell viability was measured with CCK-8 kit and presented as percentage of control group. (C) BEAS-2B cells were incubated with 2% CSE or 100 µg/ml PM2.5 for 48 hr. The levels of IL6 and IL8 in cell culture medium were determined with ELISA. Data are presented as mean ± SEM (n=5). **P < 0.01 for CS or PM2.5 group versus respective CTL group; #P < 0.05 and ##P < 0.01 for CSE group versus PM2.5 group.

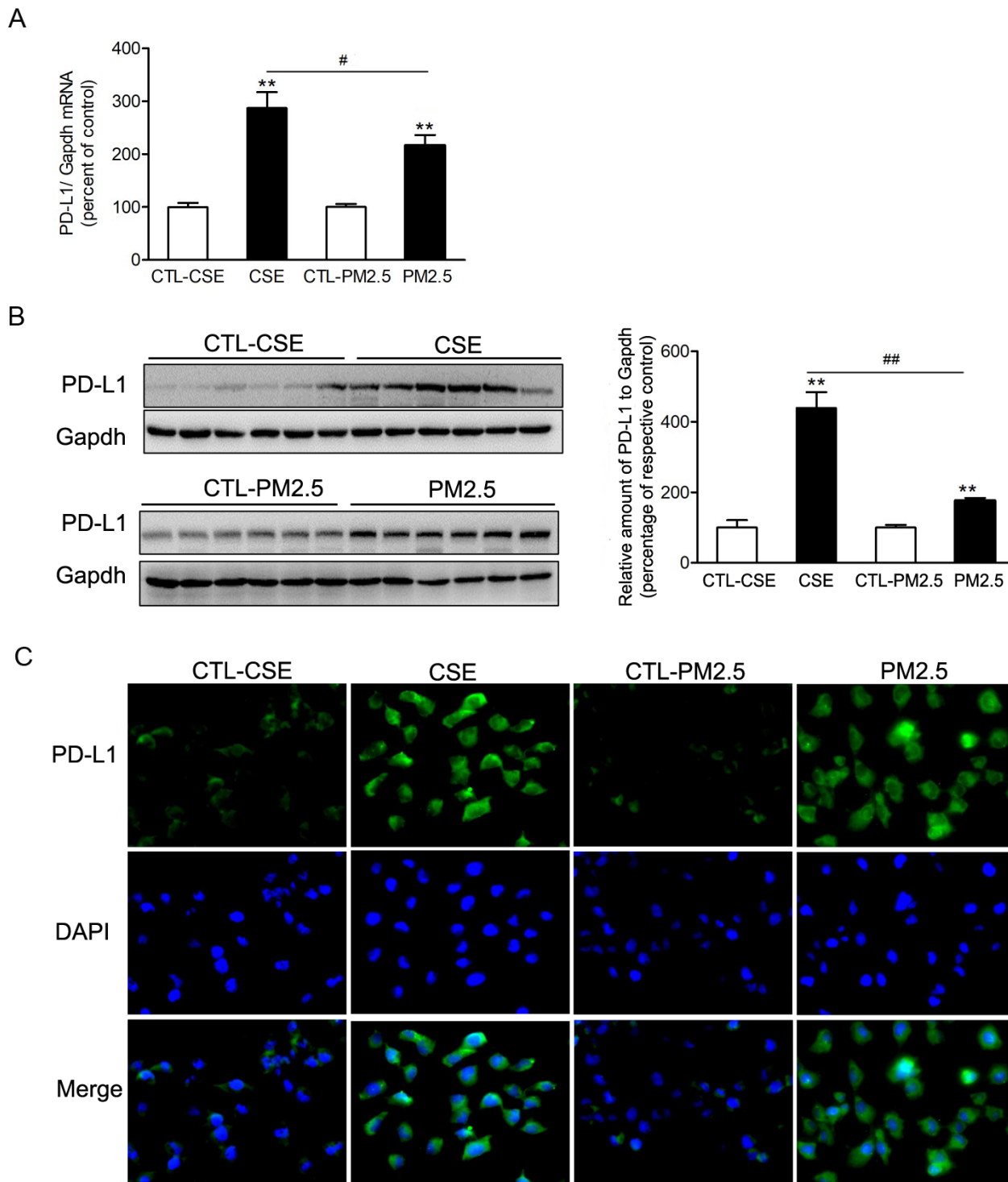


Figure 5

Cigarette smoke extract and PM2.5 induced PD-L1 increases in airway epithelial cells. BEAS-2B cells were incubated with 2% CSE or 100 μ g/ml PM2.5 for 48 hr. (A) The relative mRNA levels of PD-L1 were presented as percentage of the control cells. (B) Protein levels of PD-L1 were determined by western blotting. The blotted bands were relatively semi-quantitated to internal control (GAPDH) by densitometry and presented as percentage amount to control cells. Data are presented as mean \pm SEM (n=6). **P <

0.01 for CSE or PM2.5 group versus respective CTL group; #P < 0.05 and ##P < 0.01 for CSE group versus PM2.5 group. (C) Representative images from immunofluorescence staining of PD-L1 in cultured BEAS-2B cells.

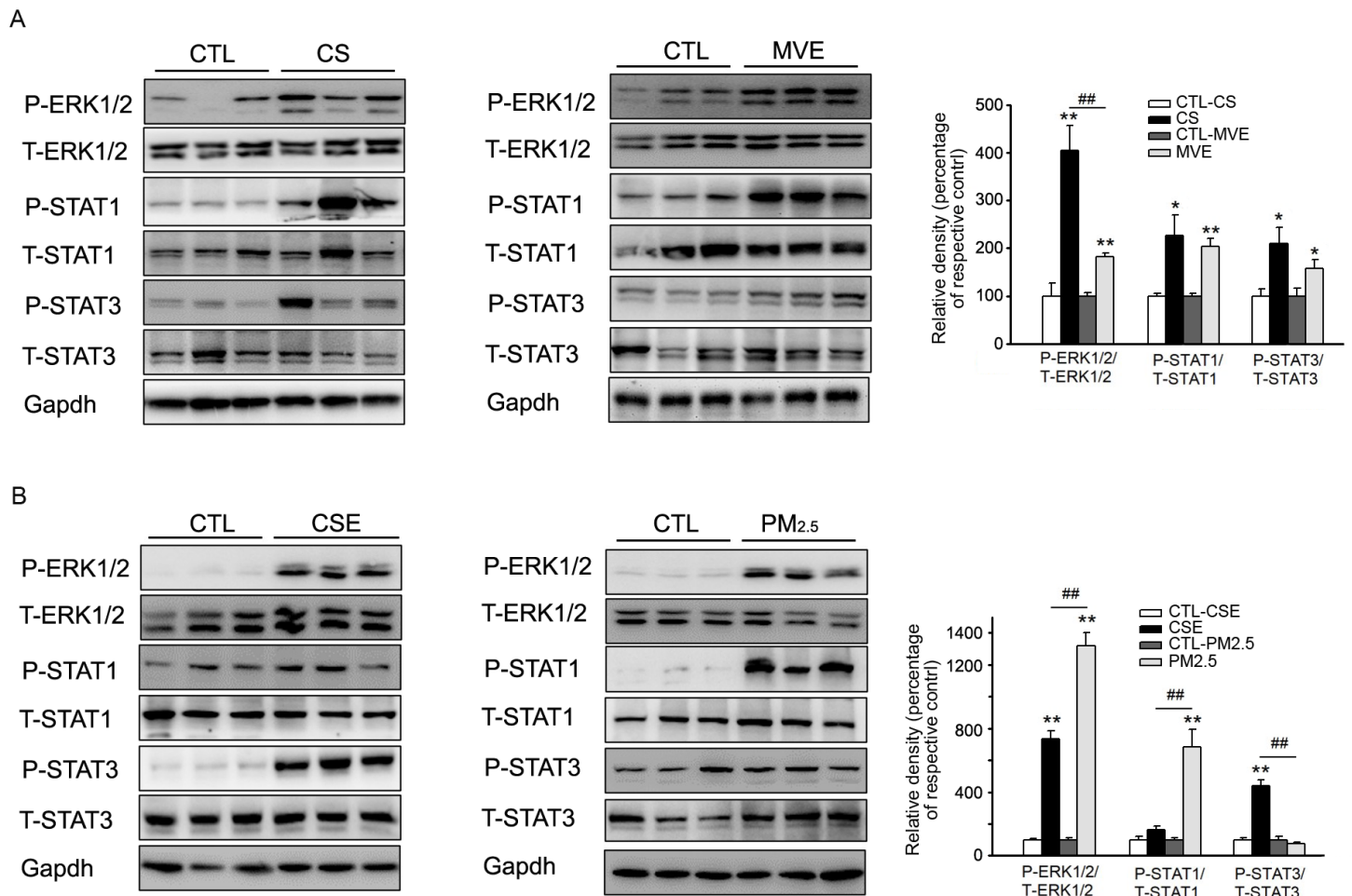


Figure 6

Phosphorylation of ERK and STAT in lung or BEAS-2B cells in respond to CS/CSE or MVE/PM2.5 treatments. Western blotting was used to determine the levels of total and phosphorylated ERK, STAT1 and STAT3 proteins in (A) lung tissues exposed to CS or MVE, or in (B) BEAS-2B cells treated with 2% CSE or 100 µg/ml PM2.5. For lung tissues, samples were randomly selected from 6 rats per group. The results for cell lysates were from one representative experiment performed in triplicates and repeated for three times. Relative semi-quantitation of the bands to internal control (GAPDH) was performed by densitometry. The ratios of phosphorylated protein to total protein were calculated and presented as percentage of respective control. Data are presented as mean ± SEM. *P < 0.05 or **P < 0.01 for CS/CSE or MVE/PM2.5 group versus respective CTL group; ##P < 0.01 for CS/CSE group versus MVE/PM2.5 group.